Characterization of the Flow Field Ahead of a Flame Propagating in an Obstructed Channel

Craig Johansen, Gaby Ciccarelli

Queen's University, Mechanical and Materials Engineering Department
Kingston, Ontario K7L 3N6, Canada

1 Introduction

Flame propagation in obstructed channels has been studied for many years, primarily in connection with explosion safety. The interaction of the flame and the unburned gas flow field generated ahead of the flame can lead to flame acceleration. This acceleration can produce local overpressures on the order of the adiabatic constant volume explosion pressure, and in the limit, can lead to the initiation of a detonation wave, commonly referred to as deflagration-to-detonation transition (DDT). This flame acceleration process is governed by several parameters including mixture reactivity and the ratio of the obstacle blockage area and the channel cross-section area [1]. In most studies flame propagation is measured down the length of the channel by ionization and photodiode probes that provide flame time-of-arrival information. Piezoelectric pressure transducers are used to record the pressure-time history at different axial locations in the channel [1]. This pressure data is used to track the development of a shock wave ahead of the flame. More recently, high-speed photography has been used to capture the complex turbulent flame shape [2]. The flame shape is dictated predominately by the unburned gas flow-field ahead of the flame. The complex flow field is dominated by turbulence flow structures produced by the obstacles, such as large eddies and shear layers. To get a better understanding of the flame propagation mechanism it is imperative to characterize this flow field for different channel geometries. In this study, a novel Schlieren based photographic technique where helium gas is injected ahead of the flame as a tracer to provide a two-dimensional map of the flow field structure ahead of the flame.

2 Experimental setup

Experiments were performed in a modular aluminum 6061-T6 combustion channel. The channel was comprised of three non-optical modules and one optical module, each with a square cross-section of 7.62cm x 7.62cm and a total length of 2.44 m. Each non-optical module is equipped with two instrumentation ports spaced 30.48 cm apart and 15.24 cm from the end flanges on both the top and bottom surfaces. The instrumentation configuration for all of the flame acceleration tests involved four piezoelectric pressure sensors mounted in instrumentation ports on the top surface. Ionization probes were mounted in each available instrumentation port on the bottom channel surface and protruded 15 mm into the test section. The ignition energy supplied to the spark plug mounted on the center of the end flange is approximately 250 mJ. The experiments were carried out with stoichiometric methane-air at an initial pressure of 47 kPa.

Flame acceleration was enhanced through an array of top and bottom-surface mounted obstacles that were distributed along the entire channel length at an equal spacing corresponding to one channel height. The effect of area blockage ratio, BR, was investigated by varying the obstacle height for three different cases (BR = 0.33, 0.5, and 0.67). In the optical module, 19 mm thick glass panels are integrated into the channel front and back sides to facilitate the visualization of the flame acceleration process through a high-speed z-Schlieren photography system. The streamwise distance between the ignition point and the first visible part of the glass is 8.255 cm. This module is equipped with a total of eight instrumentation ports spaced 15.24 cm apart and 7.62 cm from each end flange. The Schlieren system uses a 35W Xenon arc lamp and a Photron 1024 PCI high speed digital camera. The size of each Schlieren image was restricted to a height of 7.62 cm and a length of 25.4 cm, which correspond to the aluminum side cut-out length and diameter of the parabolic mirror, respectively. Schlieren images in Figure 2 are a composite of two separate but synchronized videos that were positioned side by side to create a total field of view of 7.62 cm x 44.45 cm, which corresponds to the dimensions of the entire aluminum side cut-out.

3 Visualization Technique

A novel visualization technique used in this study is the injection of a small volume of helium ahead of the flame front to act as a tracer gas in the Schlieren photographs. The helium jet is characterized by a jet diameter of 6.35 mm, a mean velocity of 3.7 m/s, and injection duration of 1 s before the initiation of combustion. As shown in the Figure 1a schematic, the helium accumulates and is partially contained in a pocket between four surface mounted obstacles before ignition occurs. The photograph in the top row in Fig. 1b represents the initial conditions just before ignition (t = 0). After ignition, the expansion of combustion products induces a flow of the unburned gas ahead of the flame, which is located to the left of the field-of-view, causing flow separation to occur downstream of each obstacle. Due to the presence of helium, the initial formation of a vortex downstream of each obstacle is visible in the second and third rows of the Schlieren photographs in Fig 1b. As the flow velocity increases with time the vortex core becomes turbulent. The vortex grows with time eventually reaching the channel side and lengthens filling the gap between adjacent obstacles to form a recirculation zone with a clearly defined turbulent shear layer, see the bottom photograph in Fig 1b.

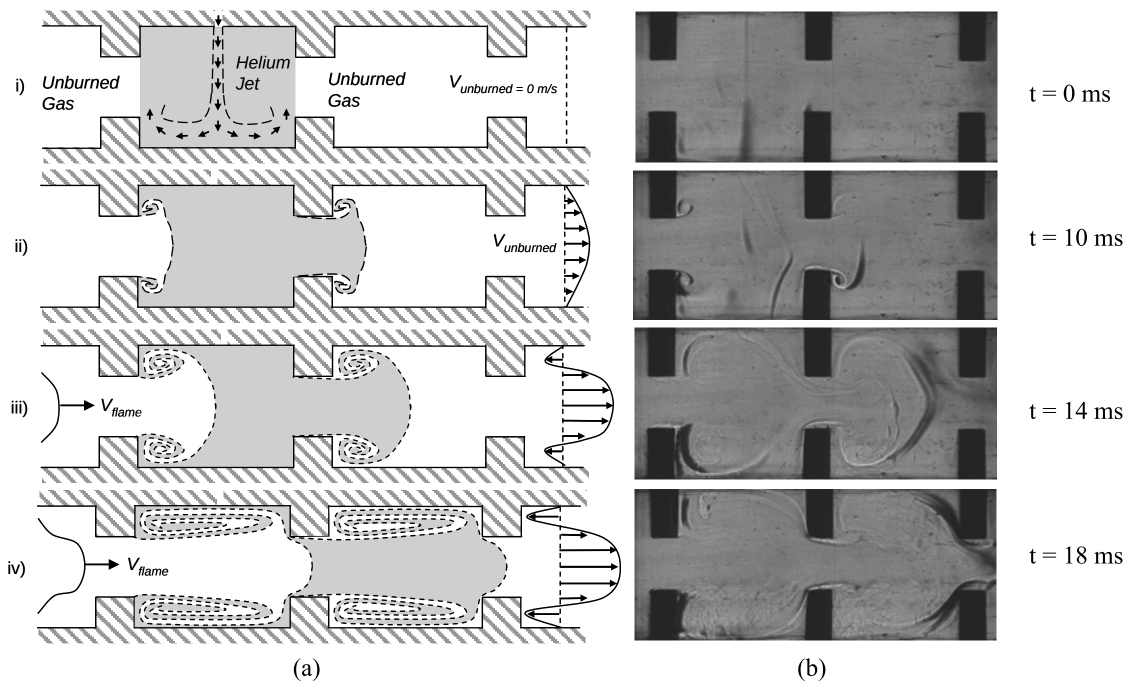

Figure 1: a) Visualization technique of helium gas injection ahead of the flame front and b) Schlieren images employing this technique (BR = 0.67, stoichiometric CH_4-Air, p_i = 47kPa)

Since flame propagation is highly dependent on the unburned gas flow field ahead of the flame that changes with time, this visualization technique gives insight into the changes observed in flame shape, combustion mode, and flame speed as it propagates from obstacle to obstacle. In Fig. 2 the Schlieren photographs show simultaneously the progression of the flame and the development of the unburned gas flow ahead of the flame for the three BR obstacles tested. Initially the flame propagates around the vortex outer surface, burning to the channel wall.

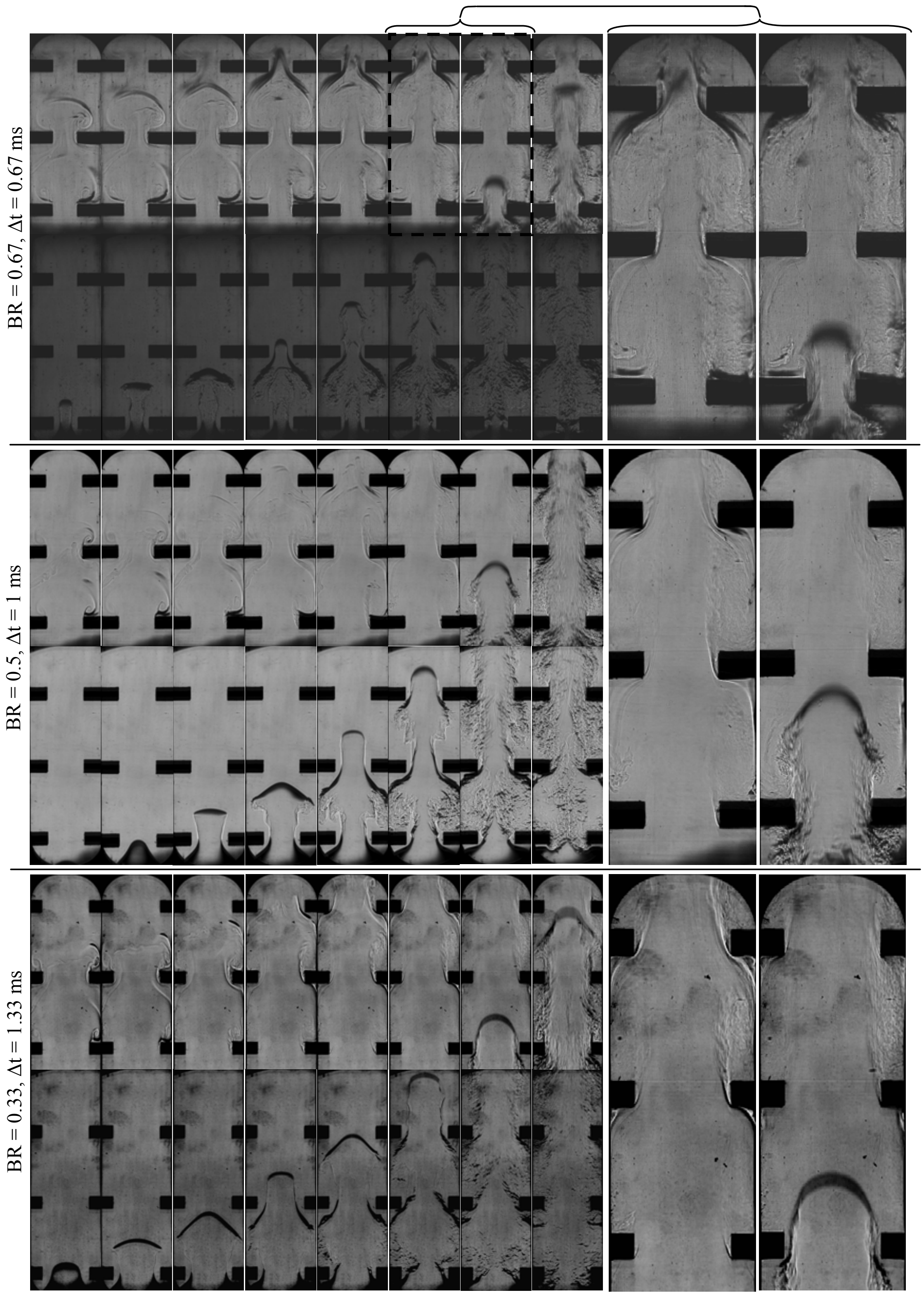

Figure 2: Effect of BR on flame acceleration and upstream flow of stoichiometric CH_4-Air (p_i = 47kPa, $\Delta t_{BR=0.33}$ = 1.33ms, $\Delta t_{BR=0.5}$ = 1ms, $\Delta t_{BR=0.67}$ = 0.67ms)

This results in a "mushroom" shape flame tip. The diverging flow area between the vortex pairs causes the flame centerline-velocity to decrease and then increase as the flow contracts through the next obstacle pair. This early stage centerline flame velocity oscillation is observed in Fig. 3a. For higher blockage ratios the velocity oscillations grow with streamwise distance, while for lower blockage ratios the velocity oscillations diminish. For later stages of the flame acceleration, the flame cannot immediately reach the duct wall resulting in a long and narrow flame shape where propagation in the streamwise direction is dominant. Just before the flame leaves the field-of-view (see the magnified bottom photographs in Fig 2) it appears that the turbulence has not spread to the centerline of the channel and the flame tip is still laminar (unfortunately the flame velocity is too high for the camera shutter speed so the flame tip appears slightly smeared but smooth). It is possible that before compressible effects, the core flow remains laminar due to the high Reynolds number and short time available for the shear layers to spread towards the channel centerline.

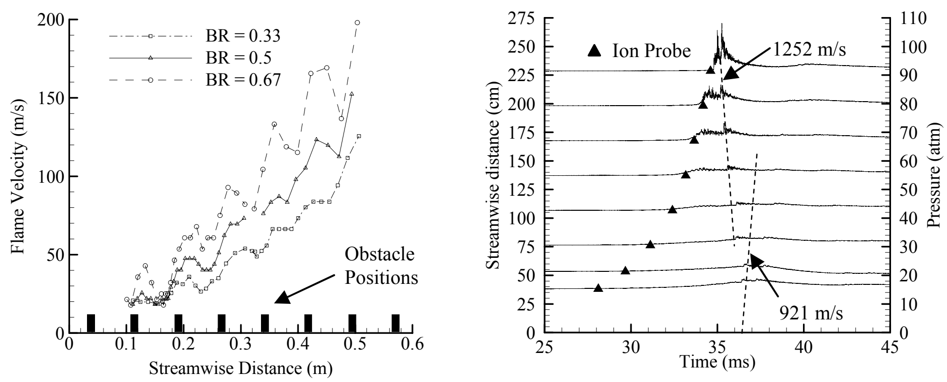

(a) (b)

Figure 3: a) Flame velocity vs. distance for different BR and (b) pressure traces and flame time of arrival data corresponding to sensors positioned down the length of the channel (BR = 0.33)

The higher flame acceleration observed in Fig. 3 for the higher blockage ratio obstacles is due to two factors associated with the flame volumetric burning rate. In the initial "mushroom" stage of flame propagation, because of the higher flow contraction through the higher BR obstacles, a higher unburned gas centerline velocity is generated that results in more elongation of the flame tip and thus a larger flame surface area. In this initial stage the flame is essentially laminar so the volumetric burning rate is governed solely by the flame area. In the later stage of propagation observed in Fig. 2 for the lower BR obstacles, most of the flame front is located at the "laminar" flame tip and the pockets of gas between the obstacles that burn via turbulent combustion are consumed quicker than the larger BR obstacles that have deeper pockets. As a result, the overall volumetric burning rate is higher for the larger BR obstacles which results in enhanced early flame acceleration. For the combustion in the first channel module (roughly 50 cm long) shown in Fig. 2, the pressure in the vessel is roughly uniform and there are no shock/flame interactions. Figure 3b shows that a finite-amplitude compression wave starts to develop ahead of the flame at roughly mid-span of the channel. The reflection of this compression wave off the obstacles and the subsequent interaction of the reflection waves and the flame lead to Rayleigh Taylor flame instabilities and further flame acceleration. This compression wave eventually reaches the channel end wall and reflects back towards the ignition end.

References

[1] G. Ciccarelli, C. Fowler, M. Bardon (2005). Effect of obstacle size and spacing on the initial stage of flame acceleration in a rough tube, Shock Waves 14(3): 161-166.

[2] M.S. Kuznetsov, I.D. Matsukov, V.I. Alekseev, S.B. Dorofeev (1999). Photographic study of unstable turbulent flames in obstructed channels, 17th International Colloquium on the Dynamics of Explosions and Reactive Systems, Heidelberg, Germany.